Peak Factors for Non-Gaussian Load Effects Revisited

Dae Kun Kwon and Ahsan Kareem

NatHaz Modeling Laboratory, Department of Civil Engineering and Geological Sciences,

University of Notre Dame

dkwon@nd.edu; kareem@nd.edu

ABSTRACT

The estimation of the extreme of non-Gaussian load effects for design applications has often been treated tacitly by invoking a conventional peak factor based on Gaussian processes. This assumption breaks down when the loading process exhibits strong non-Gaussianity, where a conventional peak factor yields relatively nonconservative estimates due to failure to include long tail regions inherent to non-Gaussian processes. In order to realistically capture the salient characteristics of non-Gaussian load effects and reflect these in the estimates of their extremes, this study examines the peak factor for non-Gaussian processes, which can be used for estimating the expected value of the positive and negative extremes of non-Gaussian load effects. The efficacy of previously introduced analytical expressions for the peak factor of non-Gaussian processes based on a moment-based Hermite model is evaluated and the variance of the estimates in terms of standard deviation is derived. In addition, some improvements to the estimation of the peak factor and its standard deviation are discussed. Examples including immediate applications to other areas illustrate the effectiveness of this model-based peak factor approach.

Keywords: Peak factor; Non-Gaussian process; Wind pressure; Buildings, low-rise; Wind loads; Probability density functions; Structural response; Structural safety.

INTRODUCTION

The assurance of the safety and reliability of structures requires accurate estimation of the extremes of the externally applied load effects due to winds, waves and earthquakes. If the statistical description of input and/or output in a system differs significantly from Gaussian, conventional methodologies with implicit assumptions of Gaussianity may no longer be valid, requiring a non-Gaussian estimation framework. This is particularly important when considering the extremes, which are sensitive to the tail regions of the probabilistic description of non-Gaussian processes, e.g., pressure fluctuations in separated flow regions (Kareem et al. 1995).

Customarily, in the area of wind effects on structures, peak factors for Gaussian processes (Davenport 1964) have been widely used in most codes and standards to estimate the expected extremes of wind loads and the related response for design applications, e.g., acceleration response of tall buildings [Fig. 1(a)]. However, this factor generally yields nonconservative values when applied to non-Gaussian processes, e.g., a time history of wind pressure fluctuations around low-rise buildings [Fig. 1(b)]. To overcome this shortcoming, Kareem and Zhao (1994) proposed an analytical form of a univariate non-Gaussian peak factor. Despite its usefulness in predicting extremes of non-Gaussian processes, some ambiguity remains regarding robustness of its application. This ambiguity may be due to a lack of consistent descriptions of some of the parameters involved, which

may be partially due to the fact that the factor was derived based on various background theoretical considerations (Rice 1944, 1945; Cartwright and Longuet-Higgins 1956; Davenport 1964; Grigoriu 1984; Winterstein 1985, 1988). This has led to a few studies that have inadvertently utilized this formulation with incorrect interpretation of the formula which led to potentially misleading conclusions. This has prompted the writing of this paper for correctness and consistency in the use of the approach (Pillai and Tamura 2007; Binh et al. 2008).

In this study, a non-Gaussian peak factor by Kareem and Zhao (1994) is revisited to clarify its background and suggest a corrected expression and demonstrate its effectiveness with additional refinements. In addition, the standard deviation of the non-Gaussian peak factor estimate is derived, which due to large variability in the peak value estimates is believed to be of higher significance than that of its counterpart in Gaussian processes.

THEORETICAL BACKGROUND

The theoretical background involved in the derivation of the non-Gaussian peak factor expression (Kareem and Zhao 1994) is briefly reviewed for the sake of completeness. Note that for consistency, the random variable x represents unconditioned data, whereas y denotes its standardized (normalized) version derived as $y = (x - \bar{x})/\sigma_x$, where $\bar{x}, \sigma_x$ = mean and standard deviation of a process x, respectively. In addition, kurtosis (γ_4) is here defined as 'normalized 4th central moment of a process – 3' so that γ_4 reduces to zero for Gaussian processes, i.e., 'excess kurtosis'. Finally, this study focuses on the softening process for which kurtosis of a standardized process is larger than zero: $\gamma_4 > 0$.

Conventional peak factor for Gaussian processes

A well-known conventional peak factor for Gaussian processes (Davenport 1964) was derived based on the distribution of the maxima (positive and negative) of the standardized Gaussian processes (Cartwright and Longuet-Higgins 1956) in conjunction with the cumulative distribution function (CDF) of the extreme and an expression for the expected number of maxima $\bar{N}$ due to Rice (Rice 1944, 1945) (e.g., Appendix I). Using the probability density function (PDF) of the extreme (Eq. 1), the expected extreme, i.e., peak factor (g_G), and its standard deviation (σ_{g_G}) were derived (Davenport 1964):

$$p_{ext}(y) = \exp(-\psi)\frac{d\psi}{dy}, \quad \psi = \nu_0 T \exp\left(-\frac{y^2}{2}\right) \tag{1}$$

$$g_G = \int_0^\infty y(\psi)\exp(-\psi)\,d\psi \approx \beta + \frac{\gamma}{\beta}, \quad \sigma_{g_G} = \frac{\pi}{\sqrt{6}\beta} \tag{2}$$

where $p_{ext}(y)$ = PDF of the extreme of a standardized process y; $\nu_0 = \sqrt{m_2/m_0}$; $m_i = i^{\text{th}}$ spectral moment ($= \int_0^\infty n^i S_y(n)\,dn$); $S_y(n)$ = one-sided power spectral density (PSD) of y; n = frequency in Hertz; T = duration of y in second; $\beta = \sqrt{2\ln(\nu_0 T)}$; γ = Euler's constant ($\approx$ 0.5772). In this derivation, some assumptions were invoked: 1) the total number of maxima is large; 2) the threshold level of the extreme is large; and 3) a Poisson based approximation that the crossings over a level are assumed to be independent of each other. The preceding first two conditions are satisfied in most cases when sufficient data points are available. The Poisson approximation, however, can be argued as, among others, Vanmarcke (1975)

has pointed out that this assumption may become conservative, especially for very narrow-band processes in which clustering effects may occur and the independence assumption may no longer be valid due to the near periodic nature of the process along with a dominant frequency. Other work, based on extensive simulations of narrow-band, broad-band and band-limited PSDs (Gupta and Trifunac 1998a, b), however, has shown that overall, the Poisson assumption yielded better results than those that considered clustering effects. Therefore, a conventional peak factor formula based on the Poisson assumption may still be a reasonable choice as it is usually conservative and has been widely adopted in most international codes and standards (Michaelov et al. 2001; ASCE 7-05; Huang and Chen 2008).

Translation process model for non-Gaussian load effects

Grigoriu (1984) introduced an effective model to overcome the difficulty of handling non-Gaussian processes utilizing a translation process that is derived from the underlying Gaussian process by a univariate, nonlinear transformation expressed:

$$y = \frac{x - \overline{x}}{\sigma_x} = g(u) \tag{3}$$

where $g(u)$ = a nonlinear function of u that is assumed to increase monotonically; u = a Gaussian random variable. In this manner, the mean upcrossing rate of level y of a translation process $Y(t)$, i.e., $\nu_{nG}(y)$, may be expressed as (Grigoriu 1984):

$$\nu_{nG}(y) = \nu_0 \phi\left[g^{-1}(y)\right] = \sqrt{\frac{m_2}{m_0}} \exp\left[-\frac{u^2(y)}{2}\right] \tag{4}$$

where subscript nG = non-Gaussian; ϕ [ ] = Gaussian distribution; m_0, m_2 = spectral moments of a process y based on its one-sided PSD $S_y(n)$ (thus m_0 becomes unity due to the characteristics of a standardized process y). Accordingly, the CDF of the extreme in a non-Gaussian process may be obtained from (Grigoriu 1984):

$$P_{ext,nG}(y) \cong \exp[-\nu_{nG}(y)T] \tag{5}$$

This CDF falls in the family of extreme distributions type I, known as Gumbel distribution (e.g., Ang and Tang 2006). Note that these Eqs. (4, 5) are indeed the same expressions used in the derivation of conventional peak factor (Cartwright and Longuet-Higgins 1956; Davenport 1964) except that a new random variable u is utilized instead in the translation process model.

Moment-based Hermite model

The key point of a moment-based Hermite model proposed by Winterstein (1985) is to analytically describe a nonlinear function $g(u)$ in the translation process (Eq. 3) so that the PDF of a process y becomes available in analytical form. This model consists of a cubic polynomial with coefficients, h_3 & h_4 (Eq. 6a), where the coefficients were redefined in a later publication for more accurate modeling (Winterstein 1988). The softening process ($\gamma_4 > 0$), being of greater interest, is briefly documented here.

$$y = g(u) = u + h_3\left(u^2 - 1\right) + h_4\left(u^3 - 3u\right) \tag{6a}$$

$$u(y) = \left[\sqrt{\xi^2(y) + c} + \xi(y)\right]^{1/3} - \left[\sqrt{\xi^2(y) + c} - \xi(y)\right]^{1/3} - a \tag{6b}$$

where γ_3, γ_4 = skewness and excess kurtosis of a process y, respectively; $u(y)$ = solution of Eq. (6a) for a random variable u; h_3, h_4, κ = coefficients of moment-based Hermite model (Winterstein 1988):

$$\xi(y) = 1.5b\left(a + \frac{y}{\kappa}\right) - a^3, \quad a = \frac{h_3}{3h_4}, \quad b = \frac{1}{3h_4}, \quad c = \left(b - 1 - a^2\right)^3 \tag{7a}$$

$$h_3 = \frac{\gamma_3}{4 + 2\sqrt{1 + 1.5\gamma_4}}, \quad h_4 = \frac{\sqrt{1 + 1.5\gamma_4} - 1}{18}, \quad \kappa = \frac{1}{\sqrt{1 + 2h_3^2 + 6h_4^2}} \tag{7b}$$

It is obvious that the nonlinear function $g(u)$ and/or $u(y)$ only depends on two high-order central moments, γ_3 & γ_4, which can be directly obtained from a standardized process y when the time history is available. With the Hermite model, the PDF of a standardized non-Gaussian process y can also be expressed as (Grigoriu 1984):

$$p_Y(y) = \frac{1}{\sqrt{2\pi}} \exp\left[-\frac{u^2(y)}{2}\right] \frac{du(y)}{dy} \tag{8}$$

Assuming that $u(y)$ is differentiable, the derivative $du(y)/dy$ above is analytically derived from Eq. (6b):

$$\frac{du(y)}{dy} = \frac{b}{2\kappa\sqrt{\xi^2(y) + c}} \left[\left(\sqrt{\xi^2(y) + c} + \xi(y)\right)^{1/3} + \left(\sqrt{\xi^2(y) + c} - \xi(y)\right)^{1/3}\right] \tag{9}$$

NON-GAUSSIAN PEAK FACTOR

Kareem and Zhao (1994) proposed an analytical expression for a peak factor (g_{nG}) for a non-Gaussian process, which was based on the concepts of a translation process (Grigoriu 1984), a moment-based Hermite model (Winterstein 1985, 1988) and the framework of the Gaussian peak factor (Davenport 1964) briefly reviewed earlier. Note that the original

formula in Kareem and Zhao (1994) has been subsequently utilized in later publications by the authors, Kareem et al. (1995), Gurley et al. (1997), and Kareem et al. (1998). The results lacked consistency as some parameters were defined differently and a few minor variations in both the expressions and attendant variables have been noted. A slightly different formula has also been presented in Chen and Huang (2009). In addition, it is noted in the literature that some studies have offered improvements to address issues concerning bandedness of the process and conservativeness of the results (Pillai and Tamura 2007; Binh et al. 2008). This is based on the misunderstanding in the formulation by Kareem and Zhao (1994) in which both issues were encompassed (Kwon and Kareem 2009). Thus, for the sake of clarification and casting a consistent description, the non-Gaussian peak factor is presented here with proper description of variables to preclude any further misinterpretation of the expression proposed originally in Kareem and Zhao (1994). A brief derivation of the following expression can be found in Appendix I:

$$g_{nG} = \kappa \left\{ \left(\beta + \frac{\gamma}{\beta} \right) + h_3 \left[\beta^2 + (2\gamma - 1) + \frac{1.98}{\beta^2} \right] + h_4 \left[\beta^3 + 3\beta(\gamma - 1) + \frac{3}{\beta} \left(\frac{\pi^2}{6} - \gamma + \gamma^2 \right) + \frac{5.44}{\beta^3} \right] \right\} \tag{10}$$

where β, γ, v_0, m_i defined in Eq. (2); γ_3, γ_4, h_3, h_4, κ defined in Eqs. (6) and (7). Accordingly, if the process is Gaussian the preceding equation reduces to the conventional peak factor for Gaussian processes given in Eq. (2) [γ_3 & γ_4 reduce to zero that leads h_3 & h_4 to zero and κ = 1 (Eq. 7b)]. In this manner, the conventional Gaussian peak factor in Eq. (2) may be viewed as a special case of the non-Gaussian peak factor in Eq. (10).

It is worth noting that the coefficients in Eq. (10) are computed based on the standardized process y only. For reference, strictly speaking, the spectral moments (m_i)

should be obtained from a process *u* (translation pair of a process *y*). Utilizing the spectral moments of a process *y*, however, is much more convenient in practical applications. It has been verified by several researchers (Grigoriu 1984; Tognarelli 1998; Sadek and Simiu 2002) that the error level was rather small, and thus can be neglected.

Finally, recalling that the g_{nG} is indeed the estimated extreme in a process *y*, the extreme of a process *x* should be calculated from the following expression.

$$\begin{cases} \overline{x}_{ext} = \overline{x} + g_{nG} \cdot \sigma_x & (positive\ extreme) \\ \overline{x}_{ext} = \overline{x} - g_{nG} \cdot \sigma_x & (negative\ extreme) \end{cases} \tag{11}$$

Note that Eq. (10) is formulated for the positive extremes. For negative extremes that are often observed in a time history of negative wind pressure fluctuations on the roof of low-rise buildings or sides of high-rise buildings, one of the following three options is available: a) change sign of data (i.e., data multiplied by -1); b) change sign of γ_3 (i.e., $-\gamma_3$); c) change sign of h_3 (i.e., $-h_3$). Thus, if both positive and negative extremes within a given process are of great interest, the non-Gaussian peak factor should be calculated twice: one for the positive extreme and the other for estimation of the negative extreme by invoking one of three options given above. Note that since the non-Gaussian peak factor formula in Eq. (10) always yields a positive value, a negative sign (-) is necessary to evaluate the negative extreme with the factor g_{nG} in Eq. (11).

As alluded to earlier, this peak factor formula is developed based on a combination of theoretical considerations and thus inevitably inherits their assumptions and limitations. Some comments are worth noting: 1) The peak factor formula is intended for a univariate case, i.e., single random variable. 2) The Hermite model (Winterstein 1988) was intended for mild non-stationary processes, thus the non-Gaussian peak factor may exhibit

conservative values in the case of strong non-Gaussianity. This topic is discussed further in a later chapter. 3) Only one extreme is computed at a time, i.e., non-Gaussian peak factors for positive and negative extremes for a given process are different from each other; This is necessitated as the formulation (Eq. 10) is based on models for Gaussian processes (e.g., Cartwright and Longuet-Higgins 1956; Davenport 1964), which do not require the evaluation of the two extremes due to the symmetric nature of Gaussian processes about the mean. Longer and relatively shorter tails, i.e., statistically asymmetric nature, however, are usually noted in the case of non-Gaussian processes. 4) The non-Gaussian peak factor is obtained from a single time history; thus the reliability of extreme value estimates depends on the level to which the given data set encapsulates the statistical features of the non-Gaussian process.

STANDARD DEVIATION OF NON-GAUSSIAN PEAK FACTOR

In the case of Gaussian processes it is generally acceptable to assume that the extreme is equal to the expected value of the extreme since the variability of the extreme value distribution is rather small (Davenport 1964). For non-Gaussian processes, however, this variability is rather large due to either a positive or negative tail. In addition, the observed peak may differ significantly from its expected extreme value (e.g., Sadek and Simiu 2002). This motivated the derivation of a closed-form expression for the standard deviation of the non-Gaussian peak factor ($\sigma_{g_{nG}}$). The level of $\sigma_{g_{nG}}$ may provide guidance towards establishing a procedure for estimating extremes for non-Gaussian processes. Following the

framework for the Gaussian processes by Davenport (1964), $\sigma_{g_{nG}}$ has been derived in this study (Appendix I):

$$\sigma_{g_{nG}} \approx \kappa \left[\frac{\pi^2}{6\beta^2} + 6.58h_3^2 + 9h_4^2 \left(1.64\beta^2 + \frac{12.69}{\beta^2} + 5.32 \right) + \frac{6.58}{\beta} h_3 + 6h_4 \left(\frac{2.66}{\beta^2} + 1.64 \right) + 12h_3h_4 \left(1.64\beta + \frac{2.66}{\beta} \right) \right]^{1/2} \quad (12)$$

Similar to the features of non-Gaussian peak factors given in Eq. (10), the standard deviation also reduces to $\pi / \sqrt{6}\beta$ for Gaussian processes as h_3, h_4 = 0 and κ = 1, which is identically equal to the expression for the conventional case (Eq. 2).

Accordingly, the standard deviation of the expected extreme in a process x is calculated from the following expression:

$$\sigma_{x,ext} = \sigma_{g_{nG}} \cdot \sigma_x \quad (13)$$

IMPROVEMENTS OF NON-GAUSSIAN PEAK FACTOR ESTIMATION

Although the revised non-Gaussian peak factor formulation given in Eq. (10) is based on a consistent theoretical background, one problem remains that it may yield conservative values when the process exhibits strong non-Gaussianity, e.g., relatively large skewness and/or kurtosis. This is due to the nature of moment-based Hermite models (Winterstein 1988), which were derived based on the assumption of small deviations from Gaussianity. In order to overcome this shortcoming, improvements have been suggested in the following two approaches.

Modified Hermite Model

In Tognarelli et al. (1997), a modified Hermite model was presented that facilitated an improvement in the evaluation of a non-Gaussian process y by the Hermite model of polynomial coefficients (h_3 & h_4) in the following equations:

$$\begin{aligned}\gamma_3 &= \kappa^3\left(8h_3^3 + 108h_3h_4^2 + 36h_3h_4 + 6h_3\right)\\ \gamma_4 + 3 &= \kappa^4\left(60h_3^4 + 3348h_4^4 + 2232h_3^2h_4^2 + 60h_3^2 + 252h_4^2 + 1296h_4^3 + 576h_3^2h_4 + 24h_4 + 3\right)\end{aligned} \tag{14}$$

These equations were designed simply to obtain nonlinear solutions of h_3 & h_4 by setting γ_3 & γ_4 to be equal to those of the standardized process y. These new estimates of h_3 & h_4 were then used to solve Eq. (14) to compute g_{nG} (Eq. 10) and $\sigma_{g_{nG}}$ (Eq. 12) in lieu of their original expressions in Eq. (7b). This has been demonstrated to improve the accuracy of the Hermite model and its estimation of the PDF of a standardized process y. Additional details are available in Gurley and Kareem (1997). Note that a similar technique was applied by Ditlevsen et al. (1996) to investigate the central limit convergence of the integrals of non-Gaussian fields.

Revised Hermite Model

Winterstein et al. (1994) proposed new simple expressions for h_3 & h_4 based on optimal results that minimize the lack-of-fit errors for skewness and kurtosis of the Hermite model in the earlier publication (Winterstein 1988). These expressions are intended for application in the ranges γ_3 & γ_4: $0 < \gamma_4 < 12$; $0 \le \gamma_3^2 < (2\gamma_4)/3$, which may include most cases of practical interest (Winterstein and Kashef 2000):

$$h_3 = \frac{\gamma_3}{6}\left[\frac{1-0.015\left|\gamma_3\right|+0.3\gamma_3^2}{1+0.2\gamma_4}\right], \quad h_4 = h_{40}\left[1-\frac{1.43\gamma_3^2}{\gamma_4}\right]^{1-0.1(\gamma_4+3)^{0.8}}, \quad h_{40} = \frac{\left[1+1.25\gamma_4\right]^{1/3}-1}{10} \quad (15)$$

In comparison with the modified Hermite model, this form may facilitate use in practical applications due to its closed-form expressions instead of solving coupled nonlinear equations in Eq. (14) provided its performance is equivalent to the modified Hermite model. Fig. 2 illustrates the overall procedure to estimate extremes based on the non-Gaussian peak factor framework with these improvements.

Limitation on Improvement Technique

Although these techniques are designed to improve the Hermite model, in certain cases they may violate the underlying assumption of the model as well as that of the translation process, i.e., monotonic increase of the *g*-function (Eq. 3) so that the transformation between the non-Gaussian variable *y* and the Gaussian variable *u* has a one-to-one relationship (Grigoriu 1984; Winterstein 1998; Ditlevesen et al. 1996; Tognarelli et al. 1997; Tognarelli 1998). In such a case, it may be necessary to use the non-Gaussian peak factor and its deviation without employing these improvement schemes. An advanced approach to overcome this violation may be numerical optimization of the model parameters (e.g., γ_3, γ_4) in light of a constraint condition (e.g., Tognarelli 1998). Details about the limitation and the validity of the Hermite model can be found in Tognarelli (1998). Note, however, that this violation is not observed in the following examples.

PARAMETRIC STUDY ON NON-GAUSSIAN PEAK FACTOR

To investigate the efficacy of the non-Gaussian peak factor (Eq. 10), its standard deviation (Eq. 12) and the two improvements (Eqs. 14, 15) are used with several examples involving time histories from data obtained from full-scale monitoring and wind tunnel tests. For brevity, the following abbreviations have been employed throughout these examples: HM = Hermite Model in Eqs. (6, 7); MHM = Modified Hermite Model in Eqs. (6, 7a, 14); RHM = Revised Hermite Model in Eqs. (6, 7a, 15).

Measured pressure fluctuations on a full-scale low-rise building

The first example involves measured pressure fluctuations on a full-scale low-rise building (Thomas et al. 1995) as shown in Fig. 3(a). These fluctuations exhibit quite a large departure from Gaussian (Table 1). In Fig 3(b) the histogram of the probability density functions (PDF) of the data and the respective distributions based on HM, MHM, RHM, and a Gaussian fit is shown with a zoomed lower tail region in the inset. Fig. 3(c) similarly shows the histogram of the cumulative density functions (CDF) of the data again with the respective distributions based on HM, MHM, RHM, and a Gaussian fit with a zoomed lower tail region shown in the inset. Overall, the PDFs and CDFs based on the MHM and RHM show a better fit to the histogram than the Gaussian fit and the HM. If this data were treated as Gaussian, the Gaussian peak factor and its standard deviation are respectively, 4.017 and 0.332, which are quite a bit smaller than the corresponding values of g_{nG} and $\sigma_{g_{nG}}$ given by the non-Gaussian models (Table 1). This observation reinforces that the conventional Gaussian peak factor cannot capture strong non-Gaussian features and

therefore, Gaussianity should not be tacitly assumed. As an example, the PDFs of the standardized data and its negative extreme with estimates based on RHM are shown in Fig. 3(d). The vertical lines in the extreme distribution serve as markers to indicate mean (g_{nG}) and standard deviation ($\sigma_{g_{nG}}$). For further validation purposes, the RHM-based extreme PDF [Fig. 3(d)] as well as its peak factor (g_{nG} = 7.793 in Table 1) are utilized to estimate the standard deviation of the peak factor, i.e., numerical integration of Eq. (25). This yields 1.147 for the standard deviation, which shows good agreement with the approximated result given by Eq. (12), 1.212 (Table 1).

The extreme, i.e., the largest maximum (or minimum) can also be directly observed from a single given data set, which can be used as a reference value to compare with the model-based peak factor. Depending on the characteristics of the data being analyzed, however, the extreme value estimates obtained through these models show a small deviation around the observed values due to their random nature. This is not necessarily a shortcoming of the model-based extreme estimation. Instead, this deviation may be due to use of a single time history to directly observe the extreme since it may not generally be possible in practical situations to obtain a large number of data sets for estimating extremes. The data driven models, e.g., based on MHM or RHM, offer not only stable and reliable estimates of the extreme, but also lend versatility for other applications such as simulation, fatigue estimates, structural reliability analysis etc. (Table 1).

Time histories of TLP sway and wind pressure in the roof of low-rise building model

Two types of measured standardized time histories are considered here. They include the sway response of a tension leg platform (TLP) with mild non-Gaussian response [Fig. 4(a); Table 2] and wind pressure fluctuations on the roof of a low-rise building scale model in a wind tunnel test [Fig. 4(b); Table 2]. Both examples are used for estimating negative extremes. In the case of TLP sway response, all three models (HM, MHM and RHM) lead to almost the same results as the data is only slightly non-Gaussian. Accordingly, HM may be an acceptable option in this case. MHM & RHM, however, show better PDF matches in view of the statistics of the data (Table 2) and are believed to be more accurate in estimating both g_{nG} and $\sigma_{g_{nG}}$. On the contrary, the wind pressure coefficients in a wind tunnel test (TPU: Aerodynamic database of low-rise buildings) in Fig. 4(b) exhibits strong non-Gaussianity, which results in discrepancies between HM and MHM/RHM based estimates. The observed trends are similar to the previous example.

Comparison with windPRESSURE (NIST)

windPRESSURE, a software package (NIST 2005; Main and Fritz 2006), is designed to facilitate more widespread use of the database assisted design approach for low-rise buildings. The aerodynamic database contains measured pressure time histories for a fairly large number of gable-roofed building models with a range of dimensions tested at BLWT Laboratory (Ho et al. 2003). This standalone MATLAB-based software also invokes the translation process model to estimate the extremes (Grigoriu 1984; Gioffrè et al. 2000; Sadek and Simiu 2002). Internal force time series (e.g., bending moment) obtained from the

wind pressure data in conjunction with influence functions of the structure are fitted to a Gamma distribution (for longer tail) and a Gaussian distribution (for shorter tail). The CDF of the extreme value is estimated by invoking the mapping procedure, in which its PDF (derived from the CDF) is utilized to estimate the expected extreme value (Sadek and Simiu 2002).

Accordingly, comparison with windPRESSURE results offers another data set for verifications and insights on the analytical non-Gaussian peak factor approach employed in this study. Here, one sample of the pressure database (NIST 2005) is utilized for the following building: W = 120 ft, L = 187.5 ft, H = 18 ft, R = 5ft, Open Country. windPRESSURE not only offers provision to save a selected number of time histories of the computed bending moments, but also shows extremes graphically, which is made possible by the MATLAB's zooming features (The Mathworks, Inc.). Thus, two time histories of bending moments in frame 1, which can be treated as a univariate problem, from windPRESSURE are utilized for the comparison of estimated mean extreme values based on non-Gaussian peak factor and windPRESSURE (Table 3). Two cases are considered: Case 1) at left knee, wind direction A = 15 (Fig. 5a); Case 2) at ridge, wind direction C = 165 (Fig. 5b). Overall, estimated extremes by the non-Gaussian peak factor using MHM or RHM show good agreement with those from windPRESSURE. HM yields relatively conservative extremes, but good agreement in Case 2 where its non-Gaussianity is regarded as mild, i.e., very small γ_3 & γ_4. This agrees with the underlying assumption of HM, as observed in the example of TLP sway response earlier (Table 2). Note that one discrepancy is observed in the negative extreme (or realistically a lower extreme) of Case 1, as the windPRESSURE approach uses a Gaussian distribution to estimate this extreme. To

investigate this in detail, the PDF and CDF together with a Gaussian fit and the models are shown in Figs. 6(a) and (b), respectively. The insets are zoomed in on the lower tail region of the data. It is noted that MHM and RHM exhibit very good agreements with the given data in terms of both the PDF and CDF, even in the short tail region (left-side tail). The Gaussian fit has a rather conservative tail shape (Fig. 6). Accordingly, this leads to estimating larger extreme values than those by MHM/RHM. This can also be noted through a comparison of peak factors observed by the three models: 3.88 (HM), 2.42 (MHM) and 2.42 (RHM). HM shows rather conservative tail shape compared to those of MHM and RHM in the lower tail region.

It is worth noting that although both this study and windPRESSURE employ the concept of the translation process (Grigoriu 1984), the analytical non-Gaussian peak factor and its standard deviation expression offer a more convenient format than the windPRESSURE procedure. windPRESSURE employs the Gamma and Gaussian distributions to establish the PDF of the process *y*, where the distribution parameters are estimated via the probability plot correlation coefficient method (Sadek and Simiu 2002; Tieleman et al. 2007). This study employs a moment-based Hermite model with improved schemes (MHM or RHM) to analytically obtain the PDF of a standardized process *y*. The PDF approximation with up to the fourth moment derived from the example data shows good agreement and expedience. Furthermore, windPRESSURE utilizes a point-to-point mapping procedure to estimate the CDF of the extremes, thus requiring iterations to generate the overall CDF. In addition, the PDF of the extremes is obtained from the numerical differentiation of the CDF. Consequently, the mean extreme value and its standard deviation are derived from the PDF by way of numerical integration. The model-

based approach in this study, however, can directly derive analytical forms of the CDF and PDF of the extremes, which leads to a closed-form description of g_{nG} and $\sigma_{g_{nG}}$, thus offering a more intuitive and convenient manner to estimate the expected values of the non-Gaussian extremes and their standard deviations in practical applications, i.e., simply using the closed-form expressions for g_{nG} and $\sigma_{g_{nG}}$ without following the procedure employed in windPRESSURE. Both approaches are effective in their predictions of the extremes, selection between the two may become a matter of personal choice, though for design applications closed-form expression may be more attractive.

APPLICATIONS OF NON-GAUSSIAN PEAK FACTOR FRAMEWORK

Mean Extreme Estimation for Linear Sum of multivariate non-Gaussian processes

The formulation of the non-Gaussian peak factor and its standard deviation in this study is based on the univariate, i.e., single random variable. If a non-Gaussian process Z consists of a linear sum of n-variate non-Gaussian processes X_i, i.e., $Z = \sum X_i$ ($i = 1 \sim n$), the expected extreme of the process Z ($\bar{Z}_{ext}$), may be estimated by following this expression (quadratic combination):

$$\bar{Z}_{ext} \approx \sum_{i=1}^{n} \mathrm{E}[X_i] + \sqrt{\left(\sum_{i=1}^{n} g_i \sigma_i\right)^2 + \sum_{i=1}^{n}\sum_{j=1}^{n} \rho_{ij} g_i g_j \sigma_{x_i} \sigma_{x_j}} \qquad (16)$$

where, E[ ] = the expectation symbol; ρ_{ij} = correlation coefficient between X_i and X_j, which becomes unity when $i = j$; g_i = non-Gaussian peak factor of a standardized process of X_i, which can be obtained from Eq. (10); σ_{x_i} = standard deviation of process X_i. If X_i and X_j (i

$\neq j$) are uncorrelated then ρ_{ij} is zero and the second term (square root term) reduces to the SRSS (square root of the sum of the squares) combination rule with regard to g_i and σ_i. A similar treatment can be noted in the widely established gust loading factor approach that combines the background and resonant components of response (e.g., Zhou and Kareem 2001; Kareem and Zhou 2003). As an example of this application, the formula in Eq. (16) may be applied for the estimation of peak normal stress in terms of wind load combinations in low- and mid-rise buildings (Tamura et al. 2003).

Application to non-exceedance probability level

If the extreme distribution of a non-Gaussian process can be assumed to be an extreme value type I (Gumbel) distribution, e.g., wind pressure around low-rise buildings (e.g., Sadek and Simiu 2002; Tieleman et al. 2007), then the probability level of non-exceedance can be easily estimated from the following procedure.

The Gumbel distribution consists of two parameters, which can be obtained by one of the estimation schemes:

$$F\left(x_e\right) = \exp\left[-\exp\left(-\frac{x_e - \mu}{\alpha}\right)\right] \tag{17}$$

where, $F(x_e)$ = CDF of the extreme variable x_e; μ and α = location and scale parameters, respectively. The method of moments when the sample mean and its standard deviation are available yields the following values for the parameters:

$$\begin{aligned} \alpha &= \sigma_{x,ext}\sqrt{6}/\pi \\ \mu &= \overline{x}_{ext} - \gamma \cdot \alpha \end{aligned} \tag{18}$$

where, γ = Euler's constant (≈ 0.5772); $\bar{x}_{ext}$ and $\sigma_{x,ext}$ = sample mean and standard deviation of the extreme, respectively, which can be obtained from Eqs. (11) and (13) in terms of the non-Gaussian peak factor derived in Eq. (10) and its standard deviation in Eq. (12). A typical design approach based on the mean extreme value has the non-exceedance probability level equal to 0.57 (57 %). Please note that the extreme value for an arbitrary non-exceedance probability level can be computed from Eq. (17):

$$x_e = \mu - \alpha \cdot \ln\left\{-\ln\left[F(x_e)\right]\right\} \tag{19}$$

To verify this application, an example data set involving measured pressure on a full-scale low-rise building (Thomas et al. 1995) is utilized. The CDF from the Gumbel distribution was obtained using the method of moments (Eqs. 17, 18) based on RHM and data in Table 1 and the analytical CDF based on Hermite model (Eq. 22). The CDFs show very close agreement (Fig. 7).

Non-Gaussian simulation

Assuming that a sample of non-Gaussian data is available, the moment-based Hermite model with suggested improvements can be used to simulate a univariate non-Gaussian process. A simple simulation scheme, a class of modified direct transformation (Gurley et al. 1996), is utilized here to demonstrate the simulation procedure (Fig. 8) As alluded to earlier, a moment-based Hermite model can analytically transform a standardized non-Gaussian process (y) into a Gaussian process (u) (Eq. 6a). Once the Gaussian process u is available, a Gaussian simulation scheme may be utilized such as the spectral representation method (SRM) (Shinozuka and Deodatis 1991) with known power spectral density [$S_{uu}(\omega)$],

which can be obtained from the Gaussian process u via FFT (fast Fourier transform), to generate a random sample (u_s). Finally, a realization of the simulated non-Gaussian process (y_s) can be obtained from u_s in terms of Eq. (6b).

Theoretically, extremes can also be estimated from data, if numerous data sets are available, by taking a negative or positive peak of interest from each data set. With the peaks, one can estimate the expected extreme value by simply averaging, or by constructing a PDF. In this approach, the analytical PDF (Eq. 8) based on RHM is compared to the PDF based on the peaks obtained from the above simulation scheme with the objective of investigating the efficacy of the analytical PDF as well as the accuracy of the simulation scheme. Figure 9 shows the analytical PDF and three extreme PDFs obtained from 10, 100 and 1000 simulated data sets, which are based on a measured pressure data on a full-scale low-rise building (Thomas et al. 1995). It is obvious that larger the number of peaks, the more accurate the PDF is and the closer it is to the analytical PDF. Although 1000 peaks still lack the number of points needed to accurately describe the PDF, especially in the tails, the observed trend shows good agreement with the analytical PDF.

CONCLUDING REMARKS

Extremes of non-Gaussian processes associated with winds or other natural events such as wave & seismic load effects may not be accurately estimated by a conventional peak factor typically used for Gaussian processes. This has been observed routinely in the field of wind/structural engineering, e.g., wind pressures and corresponding internal forces in low-rise buildings, where damage to roof by excursion in pressure has often been observed.

To address this for practical design perspectives, this study presents a revised non-Gaussian peak factor and its standard deviation along with additional improvement to methods for estimating extremes for univariate non-Gaussian processes. Accordingly, the conventional peak factor for Gaussian processes becomes a special case of the non-Gaussian when the terms related to non-Gaussianity are reduced to the Gaussian case. From several examples with given time histories, the efficacy of the model-based analytical peak factor approach in terms of respective improvements (MHM or RHM) for non-Gaussian cases is demonstrated. In practical applications, it may be desirable to use RHM as it involves minimum computational effort, whereas MHM necessitates the iterative solution of coupled nonlinear equations.

The extreme value estimates derived simply from data analysis may not be as robust and reliable as those derived from a data-driven model such as moment-based Hermite models. Furthermore, these models not only provide the expected value of the extreme, but also the attendant standard deviation and PDF with additional immediate applications in areas such as simulation, fatigue estimates and reliability analysis.

ACKNOWLEDGEMENTS

The authors are grateful for the financial support, in part, provided by the NSF Grant (CMMI 06-01143).

REFERENCES

American Society of Civil Engineers (ASCE) (2005). *Minimum design loads for buildings and other structures,* ASCE 7-05, ASCE, Reston, VA.

Ang, A. H-S. and Tang, W. H. (2006). *Probability concepts in engineering: emphasis on applications to civil and environmental engineering*, 2nd Edition, John Wiley & Sons, Inc.

Binh, L. V., Ishihara, T., Phuc, P. V., and Fujino Y. (2008). "A peak factor for non-Gaussian response analysis of wind turbine tower." *J. Wind Eng. Ind. Aerodyn.*, 96, 2217-2227.

Cartwright, D. E., and Longuet-Higgins, M. S. (1956). "The statistical distribution of the maxima of a random function." *Proc. R. Soc. London, Ser. A*, 327, 212-232.

Chen, X. and Huang, G. (2009). "Evaluation of peak resultant response for wind-excited tall buildings." *Eng. Struct.*, 31(4), 858-868.

Davenport, A. G. (1964). "Note on the distribution of the largest value of a random function with application to gust loading." *J. Inst. Civ. Eng.*, 24, 187-196.

Ditlevesen, O., Mohr, G., and Hoffmeyer, P. (1996). "Integration of non-Gaussian fields." *Prob. Engng. Mech.*, 11(1), 15-23.

Grigoriu, M. (1984). "Crossings of non-Gaussian translation processes." *J. Eng. Mech.*, ASCE, 110(4), 610-620.

Gioffrè, M., Grigoriu, M., Kasperski, M., and Simiu, E. (2000). "Wind-induced peak bending moments in low-rise building frames." *J. Eng. Mech.*, ASCE, 126(8), 879-881.

Gupta, I. D., and Trifunac, M. D. (1998a). "A note on statistics of level crossings and peak amplitude in stationary stochastic processes." *Euro. Earth. Eng.*, 3, 52-58.

Gupta, I. D., and Trifunac, M. D. (1998b). "A note on statistics of ordered peaks in stationary stochastic processes." *Soil Dyn. Earth. Eng.*, 17, 317-328.

Gurley, K. R., Tognarelli, M. A., and Kareem, A. (1997). "Analysis and simulation tools for wind engineering." *Prob. Engng. Mech.*, 12(1), 9-31.

Gurley, K. R., and Kareem, A. (1997). "Modelling of PDFs of non-Gaussian system response." *Proc. 7th Int. Conf. on Str. Safety and Reliability (ICOSSAR),* Kyoto, Japan.

Huang, G. and Chen, X. (2008). "Peak Factor of Wind-Excited Response Considering Influence of Bandwidth." *AAWE 2008 Workshop*, Vail, Colorado (CD-ROM).

Kareem, A., and Zhao, J. (1994). "Analysis of non-Gaussian surge response of tension leg platforms under wind loads." *J. offshore Mech. Arctic Eng.*, ASME, 116, 137-144.

Kareem, A., and Zhou, Y. (2003). "Gust loading factor – past, present and future." *J. Wind. Eng. Ind. Aerodyn.*, 91(12-15), 1301-1328.

Ho, T. C. E., Surry, D., and Nywening, M. (2003). NIST/TTU cooperative agreement - windstorm mitigation initiative: further experiments on generic low buildings, BLWT-SS21-2003, Phase 2 report.

Kareem, A., Gurley, K., and Tognarelli, M. (1995). "Advanced analysis and simulation tools for wind engineering." *Proc. 9th International Conference on Wind Engineering*, New Delhi, India, 129-140.

Kareem, A., Tognarelli, M. A., and Gurley, K. R. (1998). "Modeling and analysis of quadratic term in the wind effects on structures." *J. Wind Eng. Ind. Aerodyn.*, 74-76, 1101-1110.

Kwon, D., and Kareem, A. (2009). "Peak factor for non-Gaussian processes revisited." *Proc. 7th Asia-Pacific Conference on Wind Engineering (APCWE-VII)*, Taipei, Taiwan (CD-ROM).

Main, J. A., and Fritz, W. P. (2006). "Database-assisted design for wind: concepts, software, and examples for rigid and flexible buildings." NIST Building Science Series 180, NIST.

The Mathworks, Inc., MATLAB – the language of technical computing.

Michaelov, G., Lutes, L. D., and Sarkani, S. (2001). "Extreme value of response to nonstationary excitation." *J. Eng. Mech.*, ASCE, 127(4), 352-363.

National Institute of Standards and Technology (2005), windPRESSURE - Database-Assisted-Design software for rigid, gable-roofed building, http://www.itl.nist.gov/div898/winds/wind_pressure/wind_pressure.htm.

Pillai, S. N. and Tamura, Y. (2007). "Quasi-static Peak Normal Stress and Peak Factor." *Proc. 12th International Conference on Wind Engineering*, Cairns, Australia, 519-526.

Rice, S. O. (1944). "Mathematical analysis of random noise." *Bell System Tech. J.*, 23, 282-332.

Rice, S. O. (1945). "Mathematical analysis of random noise." *Bell System Tech. J.*, 24, 46-156.

Sadek, F., and Simiu, E. (2002). "Peak non-Gaussian wind effects for database-assisted low-rise building design." *J. Eng. Mech.*, ASCE, 128(5), 530-539.

Shinozuka, M., and Deodatis, G. (1991). "Simulation of stochastic processes by spectral representation." *Applied Mechanics Reviews*, 44(4), 191-204.

Tamura, Y., Kikuchi, H., and Hibi, K. (2003). "Quasi-static wind load combinations for low- and middle-rise buildings." *J. Wind Eng. Ind. Aerodyn.*, 91(2), 1613-1625.

Thomas, G., Sarkar, P. P., and Mehta, K. C. (1995). "Identification of admittance functions for wind pressures from full-scale measurements." *Proc. Ninth Int. Conf. Wind Eng.*, New Delhi, India, 1219-1230.

Tieleman, H. W., Ge, Z., and Hajj, M. R. (2007). "Theoretically estimated peak wind loads." *J. Wind Eng. Ind. Aerodyn.*, 95(2), 113-132.

Tognarelli, M. A., Zhao, J., and Kareem, A. (1997). "Equivalent statistical cubicization for system and forcing nonlinearities." *J. Eng. Mech.*, ASCE, 123(8), 1772-1790.

Tognarelli, M. A. (1998). Modeling of nonlinear load effects on structures. Doctoral Thesis, University of Notre Dame.

TPU, Aerodynamic database of low-rise building, the 21st Center Of Excellence program, Tokyo Polytechnic University, http://www.wind.arch.t-kougei.ac.jp/info_center/windpressure/lowrise/mainpage.html.

Vanmarcke, E. H. (1975). "On the distribution of the first-passage time for normal stationary random processes." *J. Appl. Mech.*, ASME, 42, 215-220.

Winterstein, S. R. (1985). "Non-normal responses and fatigue damage." *J. Eng. Mech.*, ASCE, 111(10), 1291-1295.

Winterstein, S. R. (1988). "Nonlinear vibration models for extremes and fatigue." *J. Eng. Mech.*, ASCE, 114(10), 1772-1790.

Winterstein, S. R., Ude, T. C., and Kleiven, G. (1994). "Springing and slow-drift responses: predicted extremes and fatigue vs. simulation." *Proc. BOSS-94*, 3, MIT, 1-15.

Winterstein, S. R., and Kashef, T. (2000). "Moment-based load and response models with wind engineering applications." *J. Solar Energy Eng.*, ASME, 122, 122-128.

Zhou, Y., and Kareem, A. (2001). "Gust loading factor: New model." *J. Struct. Eng.*, ASCE, 127(2), 168-175.

APPENDIX I. FORMULATION OF NON-GAUSSIAN PEAK FACTOR AND ITS STANDARD DEVIATION

The non-Gaussian peak factor and its standard deviation (Eqs. 10, 12) can be derived following the framework for Gaussian processes by Davenport (1964) by introducing the translation process model. For completeness, brief formulation including the translation process model is introduced here.

In terms of the distribution of the maxima of the standardized Gaussian process y proposed by Cartwright and Longuet-Higgins (1956), with the assumptions that the threshold of the extreme level and the total number of maxima are large, the PDF of the maxima can be approximated:

$$p_{\max}(y) \approx \sqrt{1-\varepsilon^2}\exp\left[-\frac{u^2(y)}{2}\right] \tag{20}$$

where $\varepsilon = \sqrt{1-m_2^2/(m_0 m_4)}$ is a descriptor of the bandwidth; m_i = in Eq. (2); u = a Gaussian random variable in the translation process model (e.g., Eqs. 3, 4). Invoking the assumption of the Poisson approximation, the CDF of the extremes may be expressed as (e.g., Eq. 5):

$$P_{ext}(y) = \exp\left[-N \cdot p_{\max}(y)\right] \tag{21}$$

where, N = the total number of maxima. For practical purpose, Davenport (1964) utilized N as Rice's expression of $\bar{N}$ instead (Rice 1944, 1945), where $\bar{N}$ is the expected number of maxima per second (= $\sqrt{m_4/m_2}$). Accordingly, N is approximated as $\bar{N}T$ (T = duration in second); thus Eq. (21) can be rewritten as follows:

$$P_{ext}(y) = \exp\left[-N \cdot p_{\max}(y)\right] \approx \exp\left[-\bar{N}T \cdot \sqrt{1-\varepsilon^2}\exp\left(-\frac{u^2(y)}{2}\right)\right]$$
$$= \exp\left[-\nu_0 T \exp\left(-\frac{u^2(y)}{2}\right)\right] \tag{22}$$

As such, the bandwidth term multiplied by N, i.e., $N \cdot \sqrt{1-\varepsilon^2}$, is reduced to a new form $\nu_0 T$ (= $\sqrt{m_2/m_0}T$), where ν_0 has often been referred to as the mean zero upcrossing rate since it has the same analytical form as half of the expected number of zeros per second (Rice 1944, 1945). By introducing a new variable ψ here, the PDF of extremes can be recast:

$$p_{ext}(y) = \exp(-\psi)\frac{d\psi}{dy}, \quad \psi = \nu_0 T \exp\left[-\frac{u^2(y)}{2}\right] \tag{23}$$

In this manner, $u(y)$ can also be expressed as a function of ψ in Eq. (23) by invoking an asymptotic expansion that retains $O(\psi^{-1})$ or greater terms as $\nu_0 T$ is usually large:

$$u(y) = \sqrt{2\ln(\nu_0 T) - 2\ln(\psi)} \approx \beta - \frac{\ln(\psi)}{\beta} \tag{24}$$

where $\beta = \sqrt{2\ln(\nu_0 T)}$ in Eq. (2). In terms of the PDF of the extreme (Eq. 23), the expected value of extremes and their standard deviation can be obtained, which leads to the non-Gaussian peak factor (Eq. 10) and its standard deviation (Eq. 12).

$$g_{nG} = \int_0^\infty y \cdot p_{ext}(y)dy = \int_0^\infty y(\psi)\cdot\exp(-\psi)\,d\psi$$
$$\sigma_{g_{nG}} = \sqrt{\int_0^\infty \left(y(\psi) - g_{nG}\right)^2 \cdot \exp(-\psi)\,d\psi} \tag{25}$$

Note that y is a cubic polynomial function of u (Eq. 6a) in the Hermite model and $u(y)$ here is treated as a function of ψ in Eq. (24), thus $y(\psi)$ also becomes a function of ψ. This

mathematical manipulation, i.e., changing y integration to ψ integration, is for the sake of convenience in the analytical integration shown in Eq. (25).

FIGURE CAPTIONS:

Fig. 1. (a) PDFs and time histories of acceleration response of a tall building; (b) PDFs and traces of surface pressure on the roof and side of a low-rise building

Fig. 2. Procedure to estimate extremes of non-Gaussian processes through a peak factor framework

Fig. 3. (a) measured full-scale wind pressure data on a low-rise building; (b), (c) PDFs and CDFs of data, Gaussian fit and three models; (d) PDFs of data and its extremes using RHM [vertical lines: mean (g_{nG}) and standard deviation ($\sigma_{g_{nG}}$) of extreme PDF]

Fig. 4. Standardized time histories (a) TLP sway response; (b) wind pressure coefficients from wind tunnel test (TPU)

Fig. 5. Time histories of bending moments in test model (NIST): (a) moment at left knee of frame 1, wind direction A = 15°; (b) moment at ridge of frame 1, wind direction C = 165°

Fig. 6. Case 1 in the NIST example: (a), (b) PDFs and CDFs of data, Gaussian fit and three models, respectively

Fig. 7. Comparison of Gumbel distribution and analytical CDF

Fig. 8. Procedure of modified direct transformation in non-Gaussian simulation

Fig. 9. Comparison of extreme PDFs obtained from analytical PDF (Eq. 8) and simulations

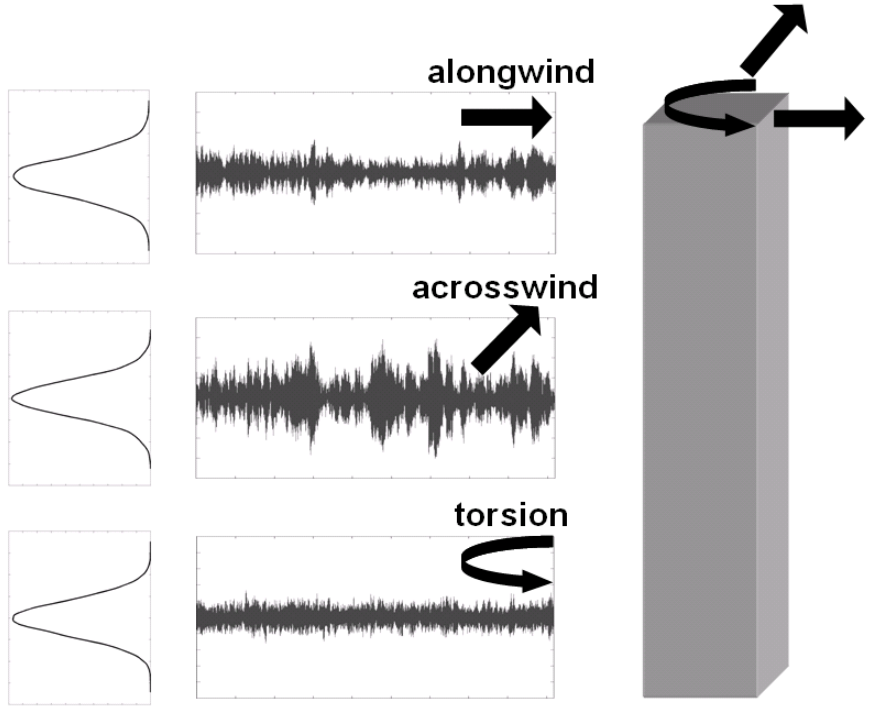

(a)

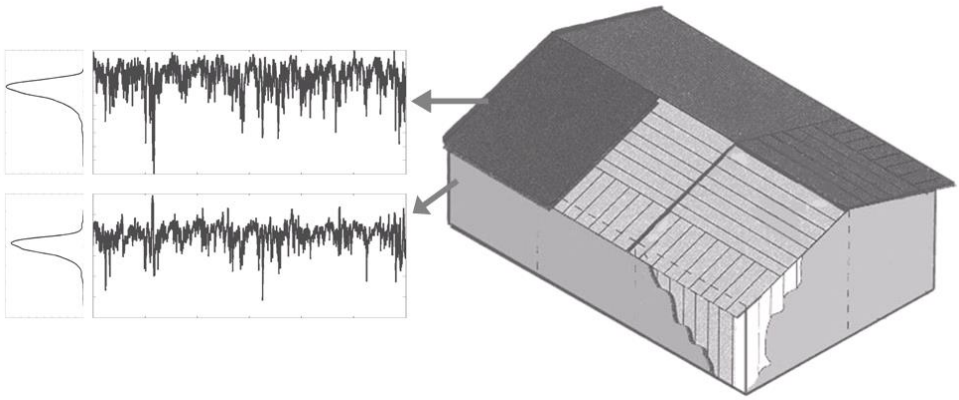

(b)

Fig. 1. (a) PDFs and time histories of acceleration response of a tall building; (b) PDFs and traces of surface pressure on the roof and side of a low-rise building

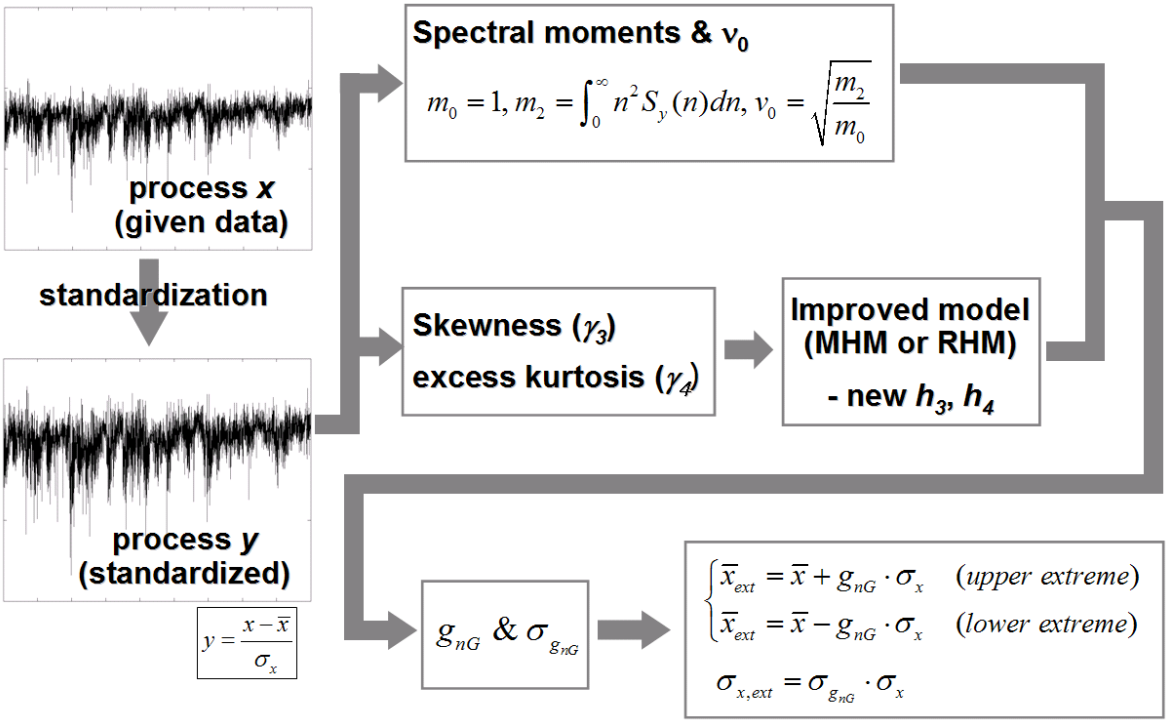

Fig. 2. Procedure to estimate extremes of non-Gaussian processes through a peak factor framework

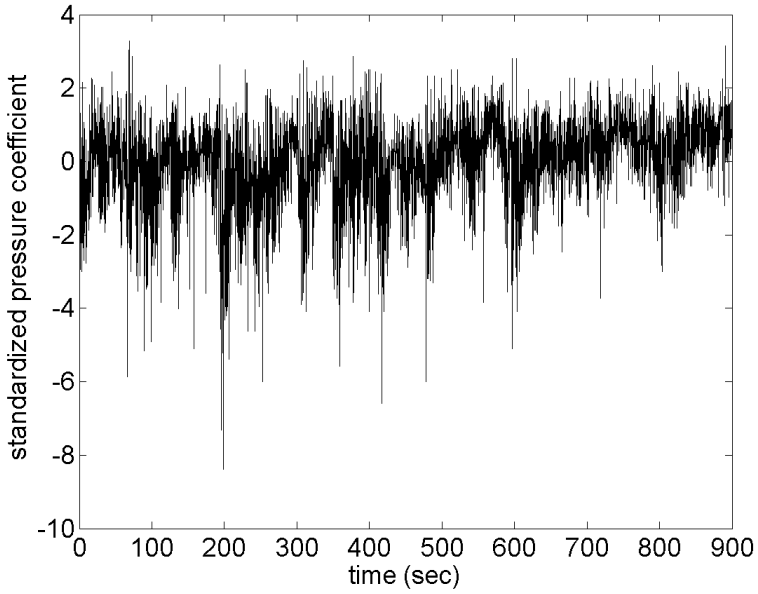

(a)

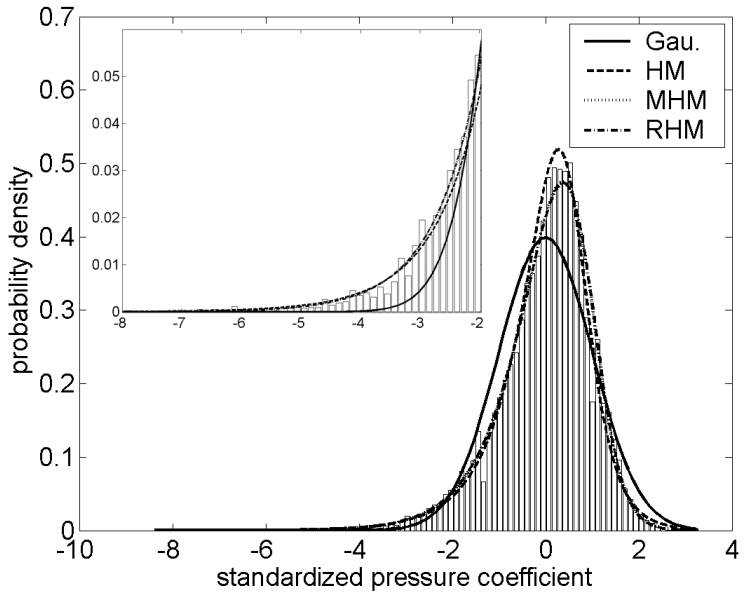

(b)

Fig. 3. (continued)

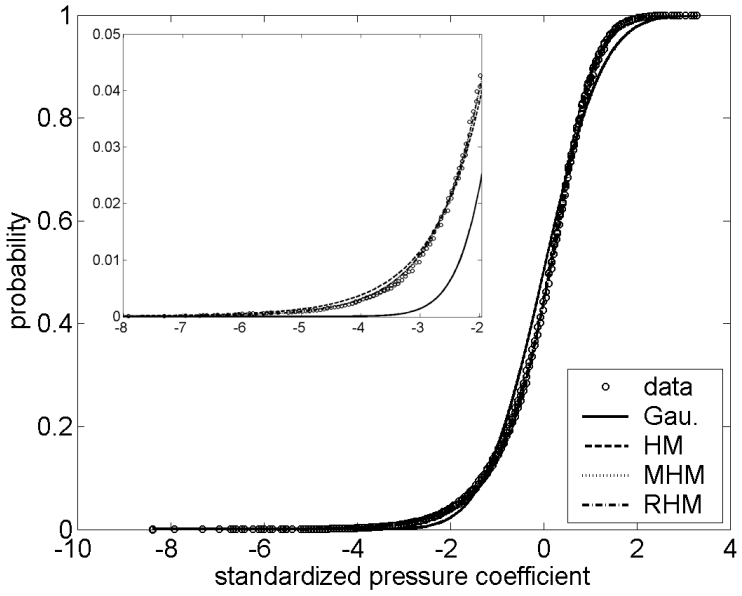

(c)

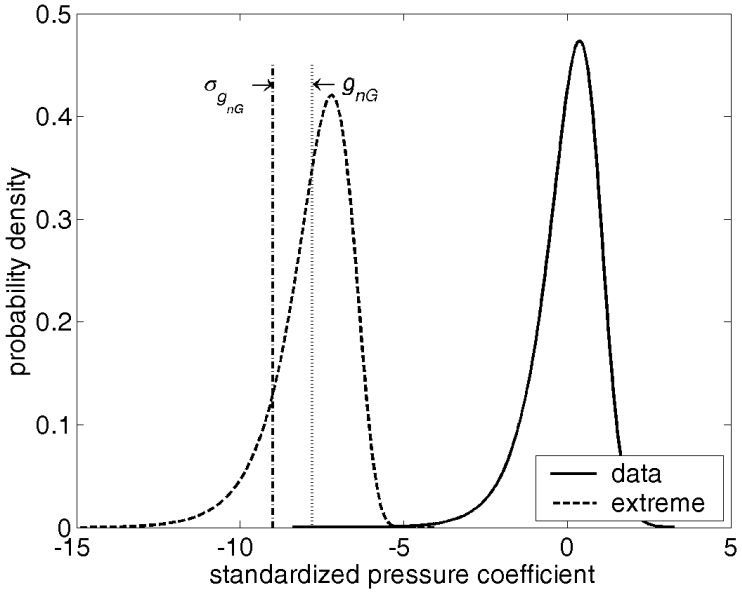

(d)

Fig. 3. (a) measured full-scale wind pressure data on a low-rise building; (b), (c) PDFs and CDFs of data, Gaussian fit and three models; (d) PDFs of data and its extremes using RHM [vertical lines: mean (g_{nG}) and standard deviation ($\sigma_{g_{nG}}$) of extreme PDF]

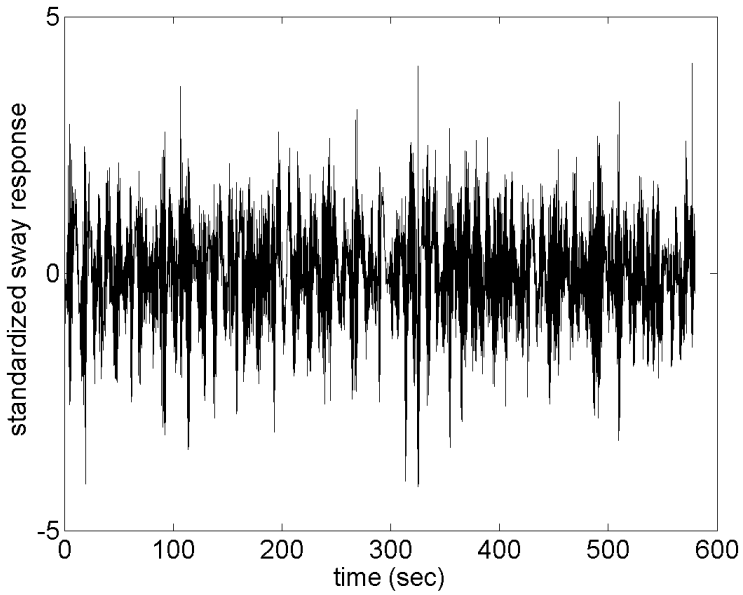

(a)

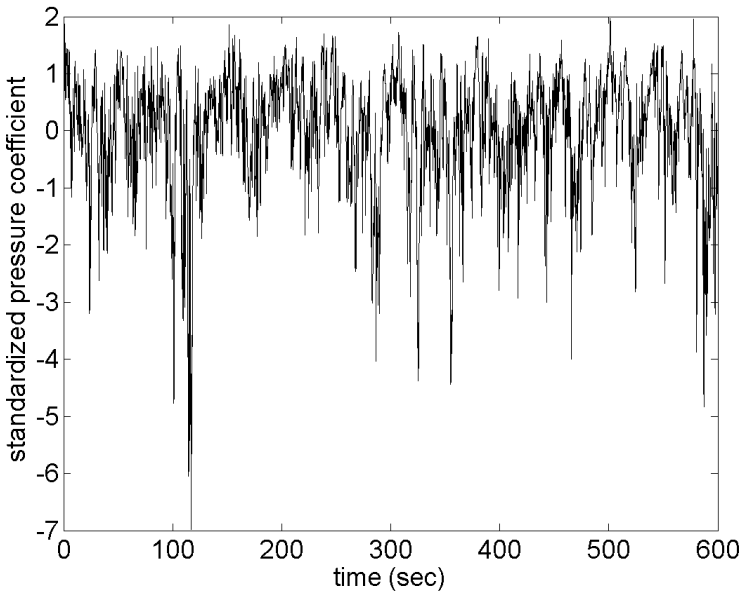

(b)

Fig. 4. Standardized time histories (a) TLP sway response; (b) wind pressure coefficients from wind tunnel test (TPU)

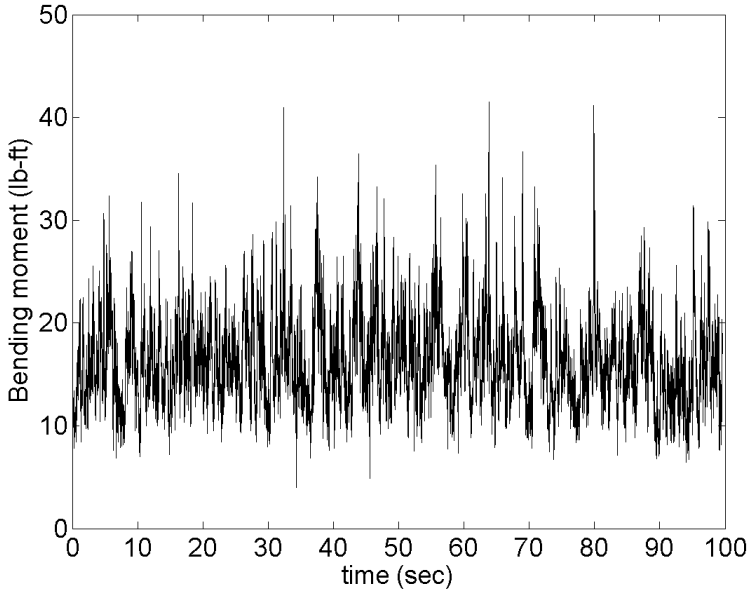

(a)

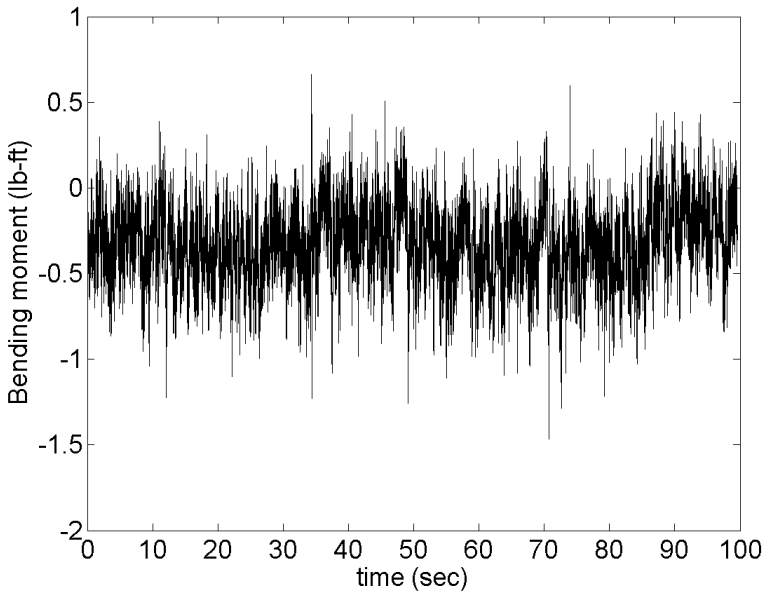

(b)

Fig. 5. Time histories of bending moments in test model (NIST): (a) moment at left knee of frame 1, wind direction A = 15°; (b) moment at ridge of frame 1, wind direction C = 165°

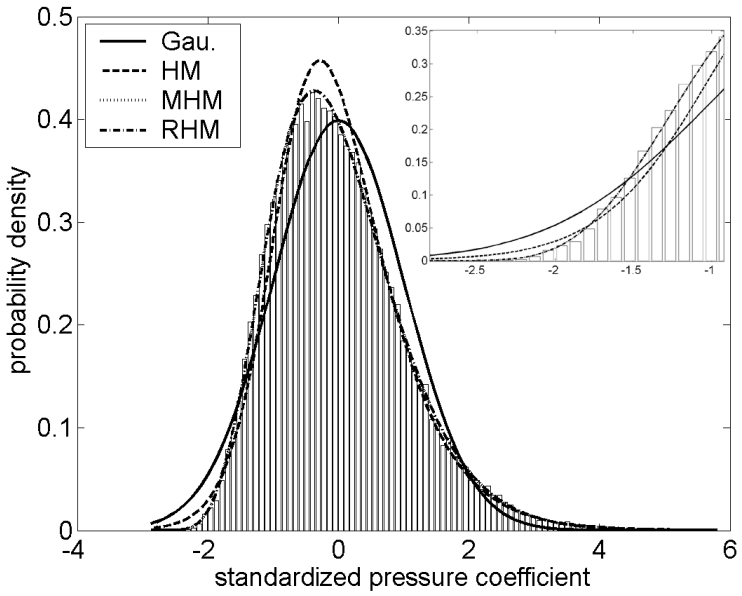

(a)

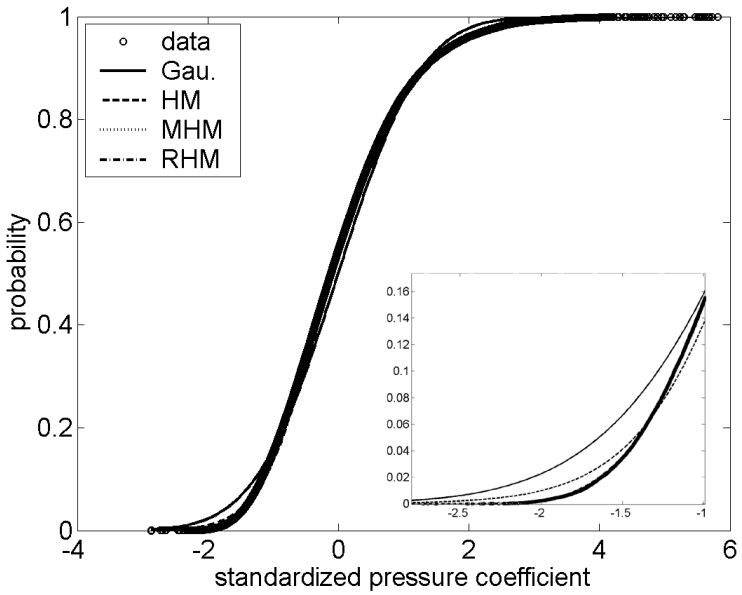

(b)

Fig. 6. Case 1 in the NIST example: (a), (b) PDFs and CDFs of data, Gaussian fit and three models, respectively

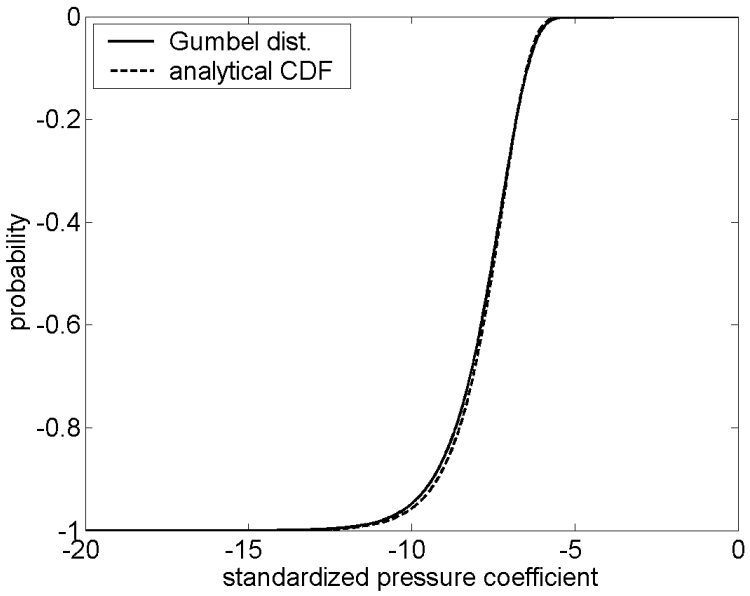

Fig. 7. Comparison of Gumbel distribution and analytical CDF

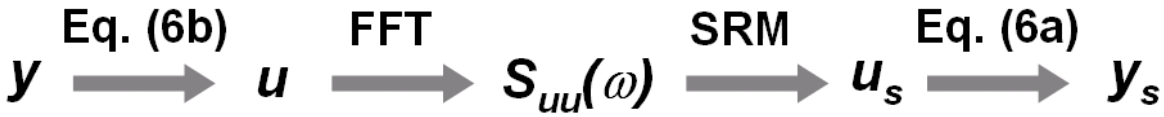

Fig. 8. Procedure of modified direct transformation in non-Gaussian simulation

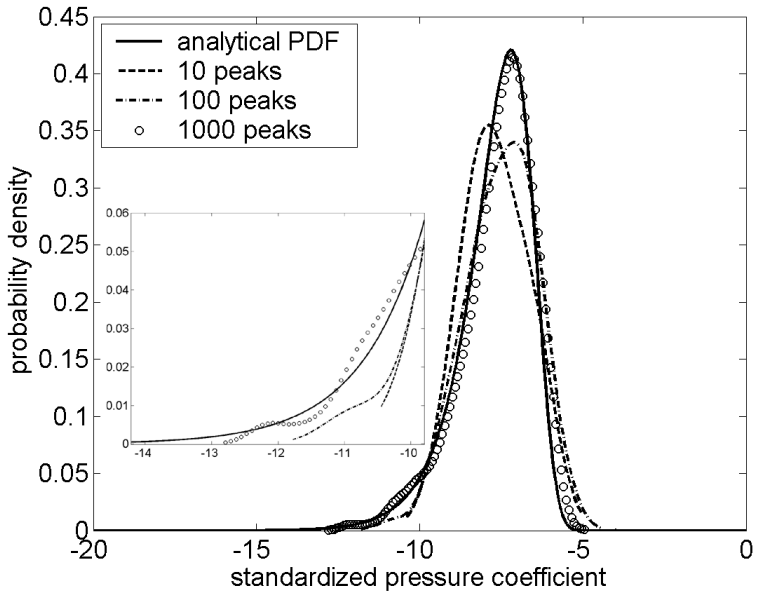

Fig. 9. Comparison of extreme PDFs obtained from analytical PDF (Eq. 8) and simulations

Table 1. Statistical values, peak factors and standard deviations from data and model-based approach (full-scale wind pressure coefficients)

	σ_y	γ_3	γ_4	g_{ng}	$\sigma_{g_{nG}}$
data	1.0000	-0.9869	2.3281	8.390[a]	–
HM	0.9970	-0.9804	3.3526	8.982	1.627
MHM	0.9997	-0.9828	2.2765	7.845	1.233
RHM	0.9999	-0.9966	2.2758	7.793	1.212

[a] observed negative extreme from standardized data

Table 2. Statistical values, peak factors and standard deviations from data and model-based approach [TLP sway response and wind pressure coefficients (TPU)]

		σ_y	γ_3	γ_4	g_{ng}	$\sigma_{g_{ng}}$
TLP Sway	data	1.0000	-0.2008	0.2976	4.147[a]	–
	HM	0.9996	-0.1967	0.3311	4.585	0.614
	MHM	0.9997	-0.1976	0.2827	4.513	0.587
	RHM	0.9997	-0.1987	0.2853	4.518	0.588
TPU data	data	1.0000	-1.4856	3.9705	6.985[a]	–
	HM	0.9768	-1.4571	5.1291	8.355	1.975
	MHM	0.9971	-1.4454	3.5492	7.148	1.422
	RHM	0.9971	-1.4725	3.5921	7.149	1.410

[a] observed negative extremes from standardized data

Table 3. Comparison of estimated extremes by model-based approach and windPRESSURE

		Standardized process			Original process			
					Pos. extreme[c]		Neg. extreme[c]	
		σ_y	γ_3	γ_4	peak	std.	peak	std.
Case 1[a]	data	1.0000	0.7639	0.9506	42.09[d]	–	4.62[d]	–
	HM	0.9922	0.7400	1.3625	46.56	4.77	-0.42	2.43
	MHM	0.9988	0.7510	0.8675	42.47	3.30	5.89	0.56
	RHM	0.9988	0.7548	0.9107	42.38	3.27	5.87	0.56
Case 2[b]	data	1.0000	-0.1428	0.1223	0.55[d]	–	-1.35[d]	–
	HM	1.0000	-0.1426	0.1490	0.58	0.076	-1.39	0.102
	MHM	0.9999	-0.1425	0.1185	0.56	0.072	-1.38	0.099
	RHM	1.0000	-0.1431	0.1253	0.56	0.073	-1.38	0.099

[a] Frame 1, Response 1 : moment at left knee, wind direction A = 15°

[b] Frame 1, Response 3 : moment at ridge, wind direction C = 165°

[c] Estimated extremes and corresponding standard deviations of bending moments [units in lb-ft]

[d] Results from windPRESSURE (Main and Fritz 2006)